Ultrafast Photoinduced Solute−Solvent Electron Transfer: Configuration Dependence

Igor V. Rubtsov,[†,‡] Hideaki Shirota,[§] and Keitaro Yoshihara*[,†]

Japan Advanced Institute for Science and Technology, Hokuriku, Tatsunokuchi 923-1292, Japan, Institute for Chemical Physics Research, Chernogolovka, Moscow Region 142-432, Russia, and Department of Chemistry and Biotechnology, Graduate School of Engineering, University of Tokyo, Tokyo 113-8656, Japan

Received: September 30, 1998; In Final Form: January 14, 1999

Ultrafast photoinduced electron transfer between excited oxazine-1 (OX1) dye and electron donating solvents aniline (AN) and *N*,*N*-dimethylaniline (DMA) has been studied with the femtosecond fluorescence up-conversion technique. Ultrafast and highly nonexponential fluorescence decay of OX1 is observed in AN and DMA. The fastest component observed is about 60 fs in DMA and assigned to fluorescence quenching due to an electron transfer reaction. Fluorescence decays are observed to be strongly dependent on the wavelength of observation in DMA and moderately dependent in AN. The wavelength dependence is assigned to fluorescence from different configurations of OX1 and solvent molecules. The energy parameters for electron transfer are estimated and discussed.

1. Introduction

The process of electron transfer (ET) is one of the most elementary processes in chemistry and biology and has been studied for a long time experimentally[1−12] and theoretically.[13−23] Several parameters of the system determine the ET rate. There are energy parameters: electronic and vibrational coupling between reactant state and product state, solvent (λ_s) and internal (λ_i) reorganization energies. There are also dynamics parameters: relaxation times for solvent and for internal degrees of freedom (usually considered as high-frequency vibrational modes). The interplay of these parameters determines different regimes of ET.

When ET is much slower than solvent dynamics, the solvent is in thermal equilibrium and the total ET rate is independent of solvent relaxation time. For faster ET the rate could be determined by solvent dynamics. When the ET rate is much faster than solvation dynamics, the solvent can be considered as frozen and the ET rate does not depend on solvent relaxation time.

A similar consideration can be made with respect to intramolecular vibrational relaxation. If the vibrational relaxation is much faster than ET, then ET occurs mainly from the relaxed vibrational states. If these times are comparable, then ET depends on the vibrational relaxation time and the ET takes place from a vibrationally excited state. For intermolecular ET processes where changing the distance between reactants modifies the ET rate, the dynamics of these changes should be considered.

When ET is intrinsically slow, diabatic potentials can be used. The ET rate in this case can be obtained by solving the Landau−Zener−Stueckelberg problem for the transmission coefficient in the crossing point of reactant and product potentials.[13−16] The two states can be strongly mixed. In this case the reaction may be understood as motion along one potential surface along the reaction coordinate where the character of the state is changing from the neutral to ionic.[17] Strong coupling leads to fast reactions which cannot be described by the diabatic approximation.

Recently, systems were found where the intermolecular ET is as fast as ∼100 fs, and much faster than diffusive solvation dynamics.[23] It was found that after photoexcitation of oxazine-type dyes, such as oxazine 1 (OX1) and Nile blue (NB), dissolved in anilines, a very fast ET occurs from the aniline molecule to the excited dye molecule.[5,24] The rate of the fast component was estimated to be ∼0.2 ps for OX1 in *N*,*N*-dimethylaniline (DMA)[24] and ∼0.1 ps for NB in DMA.[5] The formation of the products, reduced forms of the dye molecule and oxidized forms of the aniline molecule, was observed by transient absorption experiments.[25,26,29] These species have a lifetimes of several picoseconds. Very recently oscillations in transient absorption measurements with a period of ca. 55 fs were observed for OX1 in DMA and in 1-chloronaphthalene (ClNP).[29] The oscillations were assigned to the ground- and excited-state vibrations of OX1. The ET process occurred on a 30−80 fs time scale.

In this work we report our recent investigations of ultrafast intermolecular ET that highlight the processes which determine the ET rate. On the basis of improved time resolution (down to 70 fs fwhm of cross-correlation) and S/N ratio up to 10^3, we have observed a fluorescence decay of dye due to very fast intermolecular ET processes of about 60 fs. We also found that the whole process of ET is highly nonexponential in time. A distinct dependence of fluorescence decay on the wavelength of observation has been observed for the first time and is discussed in terms of fluorescence from different configurations of OX1 and solvent molecules. The observed wavelength dependence is not related to solvation dynamics.

2. Experimental Techniques

Fluorescence Up-Conversion Setup. We constructed a fluorescence up-conversion spectrometer with an instrumental response function that reaches 70 fs full width at half-maximum (fwhm). A schematic diagram of the apparatus is shown in Figure 1. An all-solid-state, homemade, Kerr-lens mode-locked, chromium−forsterite (Cr:F) laser[27] was used as a source of

* Corresponding author.
† Japan Advanced Institute for Science and Technology.
‡ Institute for Chemical Physics Research, Chernogolovka.
§ University of Tokyo.

10.1021/jp9839145 CCC: $18.00
Published on Web 03/06/1999

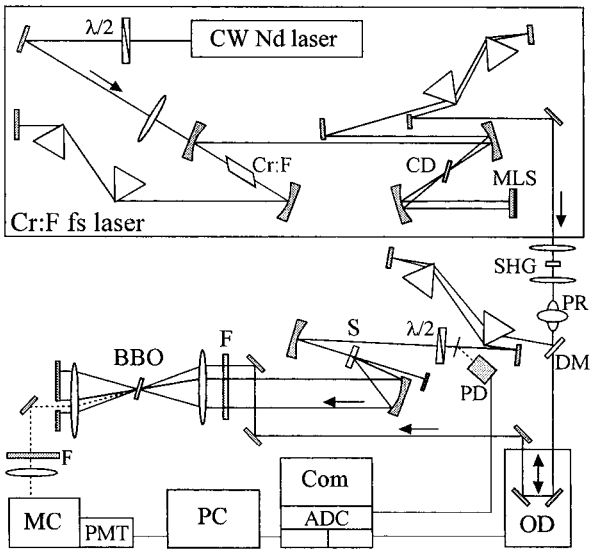

Figure 1. Schematic diagram of the femtosecond fluorescence up-conversion setup. Cr:F is a chromium forsterite crystal, CD is a cavity damper, MLS is a piezoelectric mode-lock starter, SHG is a second harmonic generation crystal, PR is a periscopic polarization rotator, DM is a dichroic mirror, OD is an optical delay line, S is a sample cell, F is a filter, BBO is an up-conversion crystal, PD is a photodiode, MC is a monochromator, and PMT is a photomultiplier tube.

femtosecond light pulses. It was pumped by a CW Nd−vanadate diode pumped laser (Spectra-Physics). The Cr:F laser works in a cavity dumped regime with a repetition rate that is adjustable from 400 Hz to 4 MHz, and produces pulses at 1260 nm with a spectral bandwidth of ∼50 nm, an energy of ∼25 nJ/pulse, and a time duration of 55 fs (fwhm).

We used an extra-cavity prism compressor, consisting of two SF6 Brewster prisms separated by 30 cm. The second harmonic (SH) was generated by a type-I process in a β-barium borate (BBO) crystal of 1.4 mm thickness. The second harmonic pulses were separated from the fundamental beam with a dichroic mirror. To obtain a large energy conversion efficiency we used a rather thick SH crystal. The SH pulse was additionally compressed with a double-pass fused silica Brewster prism pair. To minimize pulse broadening we adjusted the compressor by measuring the autocorrelation function at the position of the sample cell. The SH beam with a wavelength of 630 nm, spectral bandwidth of ∼16 nm, energy of 4 nJ/pulse, and duration of 43 fs (fwhm) was used to excite the sample. Two 100 mm radius concave aluminum mirrors were used for focusing the excitation beam onto the sample and collecting fluorescence. The fluorescence from the sample was focused in an up-conversion crystal with a 50 mm focal length lens and mixed with a gate pulse. The residual fundamental beam (∼15 nJ/pulse) after delay line was used as an up-conversion gate pulse.

As an up-conversion crystal we used a type-I BBO crystal of 0.3 or 1 mm thickness. The fwhm of cross-correlation was 90 fs for a 1 mm crystal, and 70 fs for a 0.3 mm crystal. To control accurately the instrument response function on a particular wavelength of observation, the Raman scattering signal of pure solvent was measured, which appears to be 84−90 fs depending on the wavelength.

The polarization of the pump beam with respect to the gate beam was controlled by a zero-order half-wave plate for the pump beam. The initial anisotropy value measured for OX1 in 1-chloronaphthalene (ClNP), an inactive solvent, was 0.375 ± 0.005 (less than 0.4), probably, due to imperfect polarization selection.

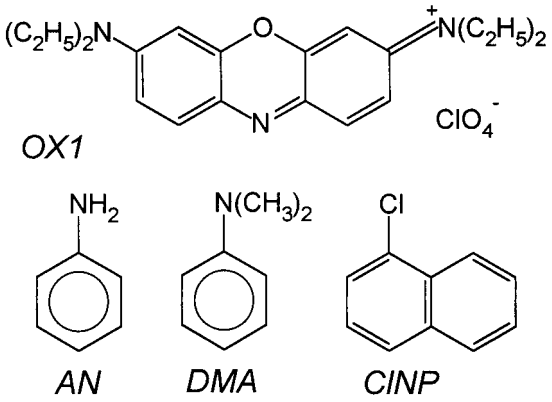

Figure 2. Molecules used in the work.

The up-converted light was directed to an aperture and focused on an entrance slit of a monochromator. The bandwidth of the monochromator was 8 nm, which corresponded to the bandwidth of fluorescence of ∼19 nm. The signal was detected with a Hamamatsu R585S photomultiplier tube cooled to −30 °C and digitized by a Hamamatsu M3148 single photon counting system. The digital signal from the photon counter was accumulated by a computer, which also controlled an optical delay line. A photodiode was used to measure the energy of SH pulses at each delay time. The signal was averaged for 1 s for one point and 3−5 data points were averaged at each time delay in one scan. We used a small step of time delay for the initial fast part of the signal (for example, 0.4 fs step for cross-correlation measurements) and increased the step when the signal changes became smaller. Once the time steps are designed this was used for other scans. Typically 1 scan consists of ∼300−400 delays. Usually 5−10 scans were averaged, each took around 20 min. For data acquisition a homemade software was used.

A 0.5 mm quartz sample cell with the walls of 0.7 mm thickness was used for up-conversion experiments. During the experiment the sample solution was circulated and kept under nitrogen atmosphere at the fixed temperature of 23 °C. The absorbance was kept around 0.5 at 630 nm, which corresponds to 10^{-4} M OX1.

The steady-state absorption and fluorescence spectra were measured by a Shimadzu spectrophotometer UV-3100 and a Jasco spectrofluorimeter FP-777, respectively. The sensitivity of the spectrofluorimeter at different wavelengths was calibrated using a standard tungsten lamp with known precise color temperature.

Chemicals. The structures of molecules used are shown in Figure 2. Solvents—aniline (AN), *N*,*N*-dimethylaniline (DMA), and 1-chloronaphthalene (ClNP)—were received from Wako Pure Chemical. All aniline solvents were distilled at least two times under vacuum, until a colorless solution was obtained, just before measurements. Oxazine-1 perchlorate (OX1) (Exciton, laser grade) was recrystallized from methanol. No change in the fluorescence decay was found after recrystallization.

Computer Simulations. The experimental data were analyzed using the "Global Unlimited" fitting program. The instrument response function of the up-conversion system was obtained from the experimental cross-correlation function or signal of Raman scattering from pure solvent. Austin Model 1 (AM1)[28] semiempirical molecular configuration calculations were performed using Hyperchem software. For optimization of configurations of $OX1^+$ and anilines^0, the restricted Hartree−

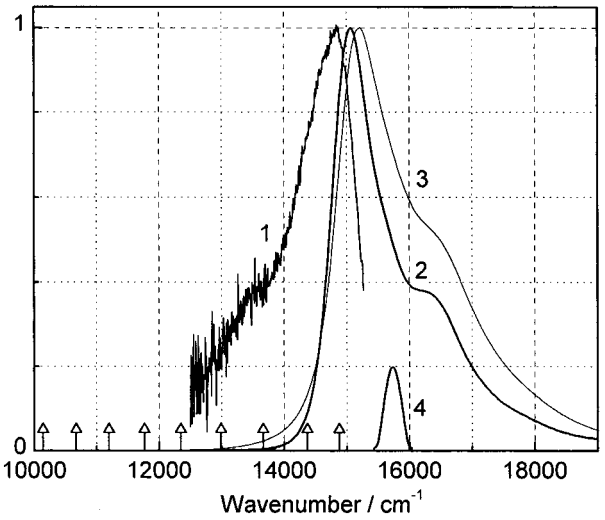

Figure 3. Steady-state fluorescence (1) and absorption (2) spectra of OX1 in AN, and absorption spectrum of OX1 in DMA (3). Spectral profile of excitation pulse (4). The arrows show the wavelengths at which the time-resolved fluorescence was measured.

Fock (RHF) method was used, for $OX1^{\bullet}$ and $anilines^{+}$ the unrestricted HF method was used.

3. Results

The steady-state absorption and fluorescence spectra of OX1 in AN and DMA (only absorption) are shown in Figure 3. The absorption spectrum of OX1 in DMA is broader than in AN. The absorption spectra of OX1 in nonpolar solvents are narrower with a more resolved vibrational progression than in AN (not shown). The broadening increase correlates with the increase of the ET rate. The wavelengths at which the fluorescence time profiles were measured are shown as arrows in Figure 3, which covers a wavelength range from 680 to 986 nm. ClNP was chosen as a "reference" solvent as it is inert (no ET), and has solvent characteristics similar to anilines, namely dielectric constant (ϵ) and refractive index (n) ($\epsilon_{AN} = 6.97$, $\epsilon_{DMA} = 4.97$, $\epsilon_{ClNP} = 5.04$, $n_{AN} = 1.586$, $n_{DMA} = 1.558$, and $n_{ClNP} = 1.632$).

Upon excitation an electron is transferred from a solvent molecule to the excited dye. For example, ET of OX1 in DMA is described as:

$$OX1^{+} \xrightarrow{h\nu} OX1^{+*}$$

$$OX1^{+*} + DMA \rightarrow OX1^{\bullet} + DMA^{+\bullet}$$

The formation of the products was observed previously by transient absorption experiments.[25,26,29] The back ET

$$OX1^{\bullet} + DMA^{+\bullet} \rightarrow OX1^{+} + DMA$$

is considerably slower ($\tau \sim 5$ ps)[26] and is not the subject of the present study.

The ET process quenches the fluorescence and determines fluorescence decay rates. In inert solvents the lifetime of excited OX1 is several nanoseconds (namely ~2.6 ns in ClNP). The fluorescence decay of OX1 is very fast in DMA (Figure 4) and slower in aniline AN (Figure 5). The improved sensitivity of our fluorescence up-conversion spectrometer allows us to detect accurately the shape of the fluorescence decay with a S/N ratio of more than 10^3. The fluorescence decay in both solvents is highly nonexponential. We approximated the time profiles with four exponentials. For example, in DMA at 732 nm the fastest component obtained by a four exponential fit is 59 fs, while

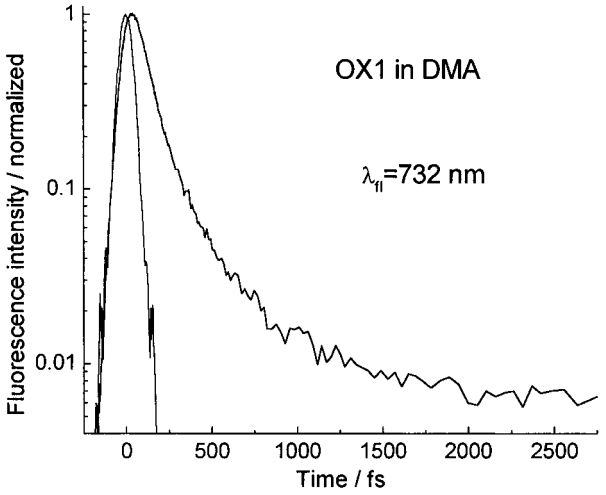

Figure 4. Fluorescence decay of OX1 in DMA in semilog scale observed at 732 nm. The instrument response measured as a Raman scattering from pure DMA at the same wavelength is also shown.

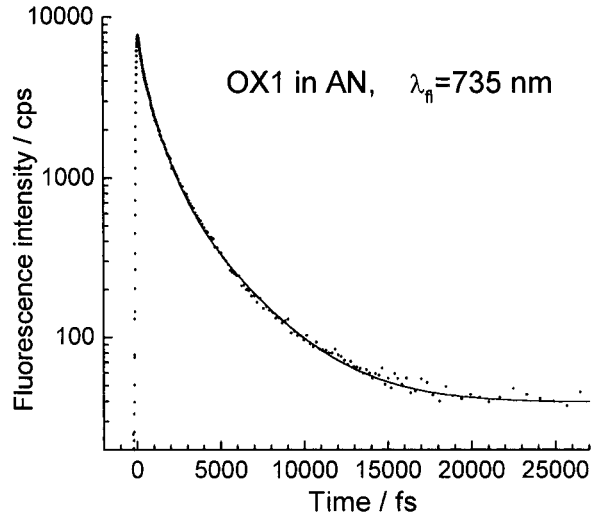

Figure 5. Fluorescence decay of OX1 in AN in semilog scale observed at 735 nm.

the slowest component is about 40 ps. The convolution of a three exponential decay with instrument response was usually made to fit the initial part of fluorescence decay since the amplitude of the slowest component is very small. The instrument response was measured carefully at the same wavelength of observation as a weak Raman scattering from the same solvent which had a fwhm of 94fs. The results of the fit are $\tau_1 = 59$ fs (80%), $\tau_2 = 200$ fs (19%), $\tau_3 = 3$ ps (1%), and $\tau_4 \sim 40$ ps (~0.3%).

A distinct dependence of fluorescence decay profile on the wavelength of observation was found in DMA (Figure 6). For example, the fast component changes from ~60 fs at 681 nm to 710 fs at 986 nm. We should emphasize that at all observed wavelengths the fluorescence decay is nonexponential, without any dominant exponential rate components. At the same time the intensities of the fluorescence signals decrease significantly toward red wavelengths (Figure 3). For example, the intensity at 986 nm is about 200 times smaller than that at 700 nm.

A moderate wavelength dependence was observed in AN (Figure 7). Almost no dependence on wavelength was observed in ClNP where no ET occurs (Figure 8). Only a very small difference was observed which is probably due to solvation. No change in the fluorescence decay profiles was observed at

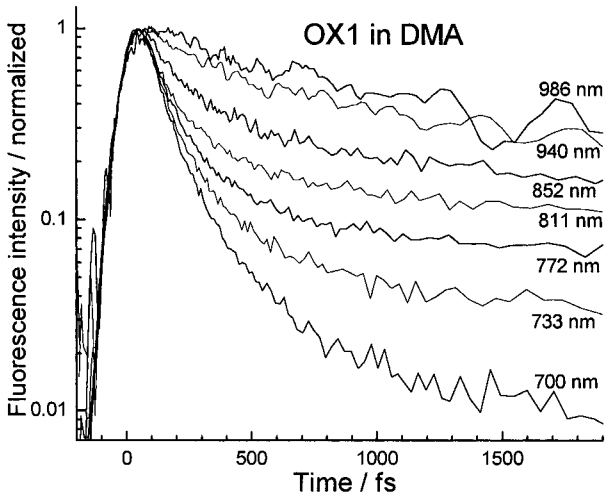

Figure 6. Fluorescence decay curves of OX1 in DMA at different observation wavelengths in semilog scale. Intensities are normalized at the peak position. The actual intensity at 986 nm is about 1/200 of that at 700 nm (see Figure 3).

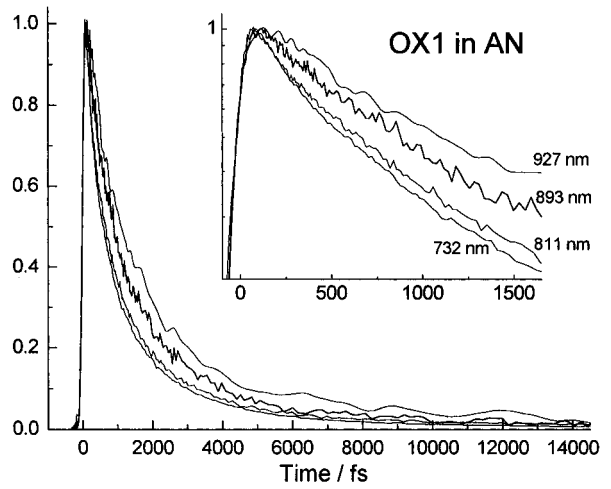

Figure 7. Normalized fluorescence decays of OX1 in AN observed at different wavelengths. In the insert, the initial part of decays are shown in semilog scale.

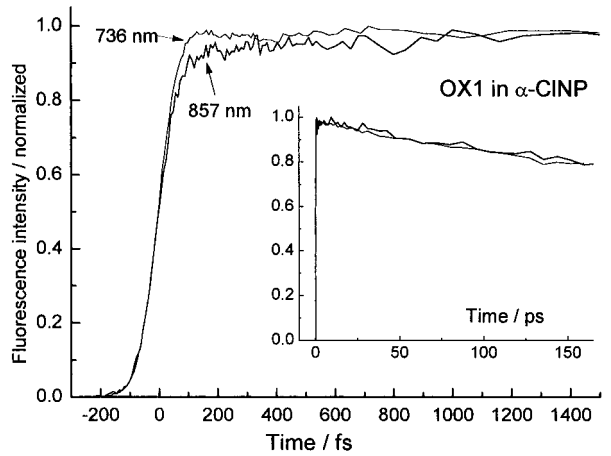

Figure 8. Fluorescence decays of OX1 in ClNP at two wavelengths, 736 and 857 nm. In the insert the long scan up to 160 ps is presented.

any wavelength upon addition of a traces of acetic acid, which confirms that fluorescence comes from monocation of OX1.

The maximum ET rate measured as the fastest component from experimental data is at least three times larger for DMA than for AN. If we discuss this in terms of an intrinsic ET rate constant[39] (maximal constant for the best mutual orientation of reactants), we can say that the intrinsic rate constants for AN and DMA differ by more than a factor of 3.

4. Discussion

The fluorescence from the local excited (LE) state of OX1 is quenched by the ET process. Although in general several relaxation processes could affect the observed fluorescence decay, such as solvation dynamics and vibrational relaxation, we will show below that the observed fluorescence decay is mainly determined by the ET rate.

4.1. Solvation of S_0 and S_1 States of OX1. The fluorescence Stokes shift of OX1 is quite small. In solvents with moderate polarity like anilines it is only about 200−250 cm^{-1}. For example in AN it is 220 cm^{-1} and in ClNP 250 cm^{-1}. OX1 is a symmetric molecule with a C_{2v} symmetry and permanent dipole moments in any states (S_0, S_1) are directed along short molecular axis z (O−N line in the central ring) (Figure 2). The difference of the dipole moments ($\Delta\mu_{S0-S1}$) is also directed along the z axis. In this case $\Delta\mu_{S0-S1}$ is usually not large (0.66 D for oxazine-4, and 0.42D for resorufin[30]—similar oxazine-type molecules with C_{2v} symmetry). As a result we expect only a small contribution from solvation dynamics in the LE state of OX1 to the observed fluorescence signal in any solvent and especially in weakly polar solvents such as anilines. Confirmation of this expectation is found in the small variation of fluorescence decay profiles observed in ClNP at two well-separated wavelengths (Figure 8).

4.2. Vibrational Relaxation in the LE State of OX1. The change of dipole moments between S_0 and S_1 states ($\Delta\mu_{S0-S1}$) is small for OX1, so the displacement of the potential curves for the ground and excited states along intramolecular coordinates is small. In this case vibrational relaxation in the LE state has a small effect on the fluorescence spectrum. This is supported by a very small wavelength dependence of fluorescence decay of OX1 in ClNP (Figure 8) where only about 20% of molecules have no high-frequency vibrations excited (judging from the analysis of the absorption spectrum).

Thus it follows that the observed fluorescence decay is determined mostly by the ET rate. The relaxation processes could affect the ET rate, but the fluorescence signal should not be changed significantly due only to these relaxation processes.

4.3. Nonexponentiality of Fluorescence Decay. The ET process in AN and DMA is highly nonexponential (Figures 4 and 5). No distinct time components of the reaction could be observed; the effective rate constant continuously decreases with time. This high nonexponentiality suggests that there is a distribution of reaction rates that arises from the initial distribution of mutual configurations of reactants. The total ET rate is composed of terms with different decay rates and gives nonexponential decay profile. Different configurations differ in distance and angle between reactants as well as in solvent surroundings. Initially there is some distribution of reactant configurations (we consider only configurations where OX1 was excited). As time proceeds the fastest configurations react quickly and slower configurations remain. Thus the ET process changes the distribution of configurations from the initial rather random distribution to a distribution where only slow pairs remain. Other processes which should be considered are the various motions of the reactants and solvent which randomize the distribution of configurations and affect the ET rate. Depending on how fast are these motions in comparison with the ET rate, the observed ET rate will give a different decay.

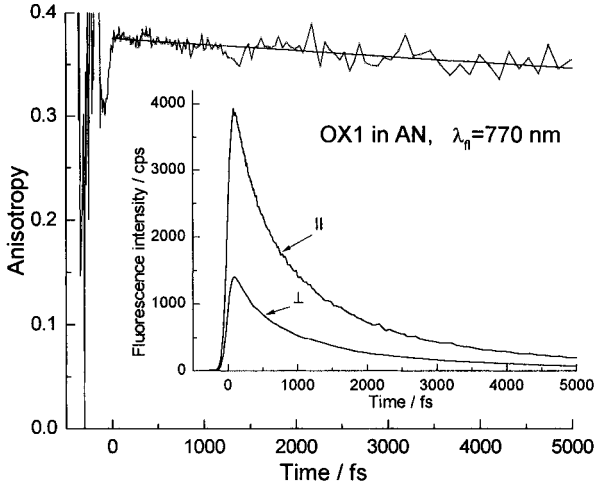

Figure 9. Fluorescence anisotropy decay $r(t)$ of OX1 in AN at 770 nm calculated as $r(t) = (I_{||} - I_{\perp})/(I_{||} + 2I_{\perp})$, where $I_{||}$ and $I_{\perp}$ are the fluorescence intensities with parallel and perpendicular polarization with respect to the excitation polarization, respectively. In the insert, the parallel and perpendicular components are shown.

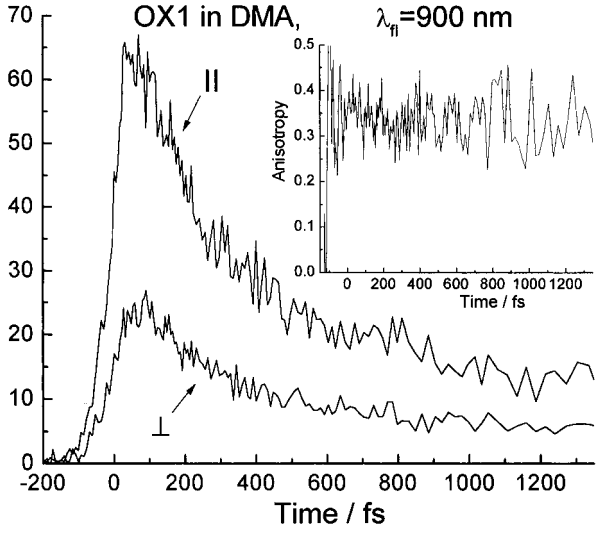

Figure 10. Fluorescence intensities (in counts per second) of OX1 in DMA at 900 nm for parallel (||) and perpendicular (⊥) polarization configurations are shown. In the insert, anisotropy decay is given.

Each motion has its characteristic time(s) which determines the time scale where that particular motion should be taken into account. For the initial time region (<300 fs), inertial motion of the reactants and solvent[31−36] should be important. The inertial motion of anilines was recently studied by optical Kerr measurements and a librational frequency of around 60 cm^{-1} was observed.[36] This corresponds to ca. 200 fs decay (overdamped regime). The fast inertial component in anilines was also suggested from dynamic Stokes shift experiments.[37]

The orientational motion of anilines is much slower with characteristic times of several picoseconds. For DMA they are 2.8 ps (71%) and 33 ps (29%) determined by optical Kerr effect[36] and 3.8 ps (46%) and 24.6 ps (54%) determined by dynamic Stokes shift measurements.[38] These motions influence the configuration distribution in the picosecond time scale.

4.4. The Wavelength Dependence. A strong dependence of fluorescence decay (of ET rate) on the wavelength of observation was found for OX1 in DMA (Figure 6), and a moderate dependence in AN (Figure 7). Almost no dependence was observed in an inert solvent ClNP (Figure 8). The fluorescence signals were observed in a very wide wavelength region, as shown in Figure 3 by arrows. We conclude that the fluorescence at all measured wavelengths is originating from the same excited state of OX1. There are two reasons for this statement. First, no change in the time course at different wavelengths was observed in ClNP (Figure 8). Second, no difference in anisotropy decay was observed for different wavelengths in all the solvents studied (Figures 9 and 10).

Upon photoexcitation the initial distribution of configurations of excited OX1 molecules is created. The initial distribution is rather random: there are "fast configurations" in which ET is fast, and "slow configurations". There are two competing processes: (a) the ET process which changes the initial distribution of configurations ("fast configurations" react quickly and only "slow configurations" remain); (b) different motions of reactants and solvent which randomize the distribution. The interplay between these two processes determines the extent of changes from initial distribution during ET reaction. If the randomization motion is faster than ET, then no changes in the initial distribution could be expected. The faster is ET the larger are the changes in the initial distribution of configurations during the ET reaction.

The absorption spectra of OX1 are broader in AN and especially in DMA than in inert solvents. The values of an additional broadening (compared with the one in ClNP) obtained from fit of absorption spectra are about 600 cm^{-1} in DMA and about 350 cm^{-1} in AN (Figure 3). The faster the ET is, the larger is the coupling between reactant (LE) and product (ionic) states and the broadening of the absorption and fluorescence spectra. This broadening has an inhomogeneous component. Different configurations give different energies of the 0−0 transition of OX1. Let us assume that the E_{0-0} energy for "fast configurations" is larger than that for "slow configurations" (vide infra). In this case the fluorescence spectrum of "slow configurations" should be located at the red compared with that of "fast configurations" (assuming that vibrational relaxation and redistribution in the excited state is sufficiently fast). The blue side of the fluorescence spectrum decays faster, as it originates from the fast configurations. The red side of the fluorescence spectrum survives longer because it arises from the slow configurations. We suggest that the observed wavelength dependence is due to fluorescence from different configurations, or it can be called configuration-dependent or site-dependent fluorescence.

If the intrinsic ET rate is relatively slow, as observed in AN, then one can expect an effective mixing of mutual configurations during the reaction by different kinds of motions (translational and orientational motions of the reactants). As a result the wavelength dependence in AN is much smaller than in DMA.

At the red wavelength edge of fluorescence in DMA, the decay has a time scale similar to that in AN. That is because for "slow configurations" in DMA, and almost all configurations in AN, the rate of the ET depends on the motions of reactants and solvent which have similar time scale in AN and DMA. In ClNP there is no ET and no wavelength dependence: the initial distribution of configurations does not change. To describe the ET of the present systems in greater detail let us estimate energy levels of the system and the free energy gap for the ET reaction.

4.5. Equilibrium Energy Levels of the Final State of ET. The energy levels of OX1−aniline pair in the aniline solvent were estimated, and the results are shown in Figure 11. On the left side of Figure 11 there are the ground and excited states of the reactants. The excited state is the LE state of the dye which we choose as the zero energy level. As mentioned above, the solvation energy is similar for ground and excited states of the

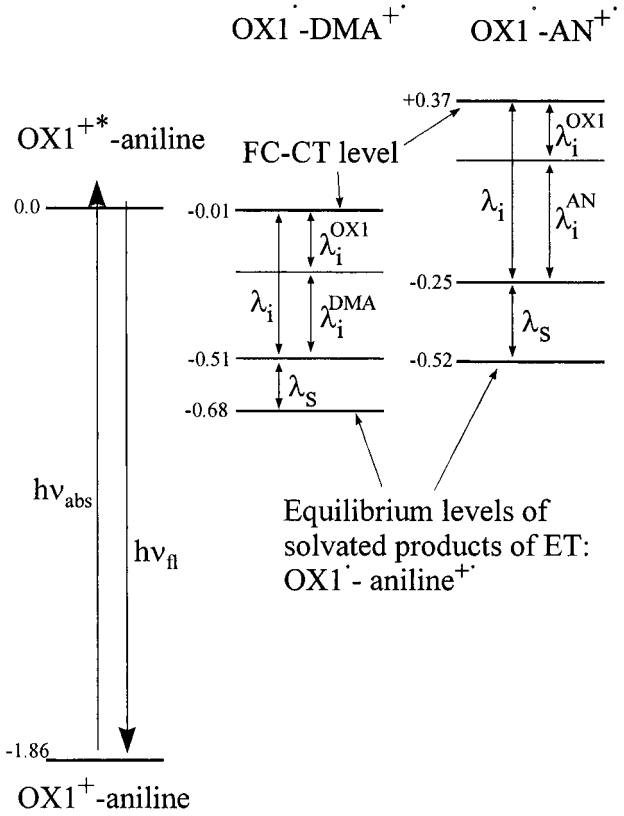

Figure 11. Energy level diagram for OX1−DMA and OX1−AN. The values of energy are given in eV.

dye, so we assume that immediately after photoexcitation the singlet excited state of OX1 is properly solvated in this system. The equilibrium energy level of the products $OX1^{\bullet} + \text{aniline}^{+}$, or in other words the free energy gap of the ET reaction, can be calculated by:

$$-\Delta G^0 = E_{00} - E(\mathrm{D/D^+}) + E(\mathrm{A/A^-}) \qquad (1)$$

where E_{00} is the 0−0 transition energy calculated from the intersection point of the steady-state absorption and fluorescence spectra (E_{00}(OX1) = 1.86 eV), E(D/D$^+$) and E(A/A$^-$) are the oxidation potential of the donor (anilines), and the reduction potential of the acceptor (OX1), respectively. Using the reduction potential of OX1 in AN: $OX1^+/OX1^0 = -0.44$ eV, and the oxidation potential of anilines: $AN^0/AN^+ = 0.93$ eV, $DMA^0/DMA^+ = 0.76$ eV in acetonitrile,[40] the following values were obtained $\Delta G^0 = -0.52$ eV for AN, and $\Delta G^0 = -0.68$ eV for DMA.

4.6. Estimation of the Reorganization Energy. To fix the displacement of the potential surface of the products with respect to the LE surface it is necessary to know the reorganization energy. The reorganization energy is the sum of two parts: the solvent reorganization energy (λ_S), due to relaxation of solvent to the product state, and the internal reorganization energy (λ_i) due to intramolecular rearrangement of donor and acceptor.

(a) Solvent Reorganization Energy λ_S. The estimate for the solvent reorganization energy λ_S can be obtained using eq 2, where reactants and products are modeled as spheres and the solvent as a dielectric continuum.[11−13]

$$\lambda_S = \frac{e^2}{2}\left(\frac{1}{r_D} + \frac{1}{r_A} - \frac{2}{l}\right)\left(\frac{1}{n^2} - \frac{1}{\epsilon}\right) \qquad (2)$$

Here, e is the unit charge, r_D and r_A are the radii of donor (anilines) and acceptor (OX1), respectively, l is the distance of the charge separation (usually distance between donor and acceptor), n the solvent refractive index ($n_{AN} = 1.586$, $n_{DMA} = 1.558$), and ϵ is the solvent static dielectric constant ($\epsilon_{AN} = 6.97$, $\epsilon_{DMA} = 4.97$). Using the values $r_{OX1} = 4.2$ Å, $r_{AN} = 2.3$ Å and $r_{DMA} = 2.5$ Å estimated from the van der Waals volumes of the molecules and the distance between OX1 and AN or DMA of 3.8 Å, we obtain the values of λ_S(AN) = 0.27 eV and λ_S(DMA) = 0.17 eV.

TABLE 1: Energy Values Calculated for OX1 in AN and DMA

	AN	DMA	OX1
ΔG^0, eV	−0.52	−0.68	
λ_S, eV	0.27	0.17	
λ_i, eV	0.41	0.29	0.21
$\lambda = \lambda_i + \lambda_S + \lambda_i$(OX1), eV	0.89	0.67	
E_{FC-CT}, eV	+0.37	−0.01	
$\Delta G^{\#}$, meV	38.5	0.04	

(b) Internal Reorganization Energy λ_i. The internal reorganization energy is due to the change of nuclear coordinates by ET. Let us assume that electron is instantaneously transferred from the donor to the acceptor. The atomic configuration of both reduced acceptor and oxidized donor still corresponds to the reagent equilibrium configuration. The difference between the energy of the initial configuration and the energy of equilibrium configuration of the products is called the internal reorganization energy. To estimate these values we have made computer simulations separately for OX1 and anilines. Let us consider this procedure for AN as an example. At first the equilibrium configuration of AN (before ET) has been determined. Then an electron was removed from it and the total energy (E_{in}) was calculated. After that the minimization procedure was performed to find the configuration of the AN^+ ion and the corresponding energy of the final state minimal energy (E_{fi}). The difference between E_{in} and E_{fi} is the internal reorganization energy λ_i ($\lambda_i = E_{in} - E_{fi}$). The same procedure was made for all anilines used and for OX1 (in this case in calculations we added an electron to the $OX1^+$ molecule). The results are shown in Table 1. The values obtained are quite reasonable: the smallest value was obtained for the OX1 molecule as it is largest molecule and can accept an extra electron without much increasing of energy. The smaller is the molecule the greater is the λ_i. The total reorganization energy λ is expressed as

$$\lambda = \lambda_S + \lambda_i(\text{aniline}) + \lambda_i(\text{OX1}) \qquad (3)$$

For Franck−Condon charge-transfer transition (FC−CT) the energy E_{FC-CT} is necessary:

$$E_{FC-CT} = \Delta G^0 + \lambda \qquad (4)$$

The results of the calculations are shown in Figure 11 and in Table 1. As can be seen from Table 1 and Figure 11, the FC−CT transition is in the vicinity of S_1—local excited (LE) level of OX1 in DMA (−0.01 eV), and much higher in AN (+0.37 eV). This means that ET in DMA could be considered as barrierless, while in AN the barrier of about $(\lambda + \Delta G^0)^2/4\lambda \sim 40$ mV is expected.

The ground-state interaction is not large (no stable complexes were observed between OX1 and anilines), so the ground-state potential energy surface is rather shallow. In this case the intermolecular distance distribution is broad. The electronic coupling strength (H_{AB}) is predicted to decay exponentially with

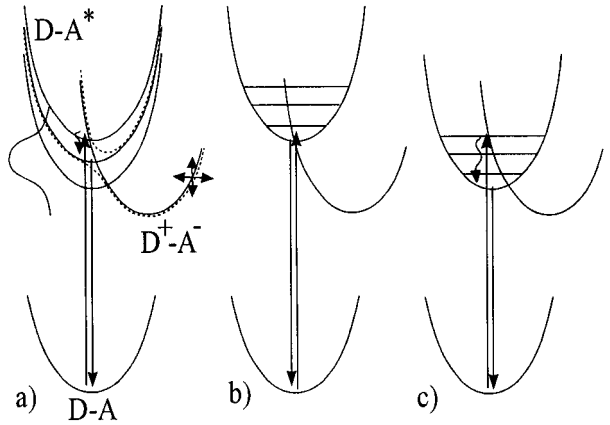

Figure 12. The energy diagram. The abscissa corresponds to reaction coordinate which is mainly internal nuclear coordinate of reactant. (a) The distribution of the configurations is presented as different traces in the excited state. The horizontal arrows on the product state represents the shift of the product energy surface due to different distances between reactants. (b) The configuration with blue-shifted fluorescence and "fast" ET is shown. c) The configurations with red-shifted fluorescence and "slow" ET is shown.

the increasing donor−acceptor separation:

$$H_{AB} = H_{AB}{}^{0} \exp\left[-\frac{1}{2}\beta(r - r_0)\right] \qquad (5)$$

where $H_{AB}{}^{0}$ is the electronic coupling at close contact (r_0), and β is the decay factor of coupling with distance. Numerous experimental studies of randomly oriented reactants have suggested $0.8 \leq \beta \leq 1.2$ Å^{-1} (refs 41, 42, and references therein). Assuming $\beta = 1$ Å^{-1}, the ET rate constant will be decreased by 1.7 times when the D−A separation increases by 0.5 Å. Another factor determining the ET rate is the orientational factor (æ) which depends on the mutual orientation of the reacting molecules. Depending on the mutual orientation of reagents æ changes from 0 to 1. Also the solvent reorganization energy is rather sensitive to the charge separation distance in the ET reaction which is considered to be the same as the distance between the reactants. If the distance between molecules changes by 0.5 Å, the λ_S changes by ca. 0.1 eV. As a result there is a broad distribution of ET rates which causes nonexponentiality of the fluorescence decay.

In some configurations one can expect that the excitation energy is sufficient to excite directly CT state (in DMA). The extinction coefficient of the CT transition is usually less than 3000 M^{-1} cm^{-1}. For our case it is probably much less than 1000, as no clear CT band was observed, so we can expect that not more than 1% of the excited molecules were excited directly to the CT state. From the experimental point of view it is manifested as a slight decrease of fluorescence amplitude, as no fluorescence from the CT state was detected on the basis of our anisotropy data.

Let us summarize the observed features. There is a distribution of configurations of reactants (including different solvent configurations). Different configurations have different ΔG^0 values. As a result, different configurations have different barriers for an ET reaction (Figure 12a) and so different ET rates give nonexponentiality. The "fast configurations" react first and the "slower configurations" remain. In Figure 12, two cases are shown. In Figure 12b, the configuration corresponds to a higher E_{0-0}. In this case the state that corresponds to the 0−0 transition is excited. As a result, ΔG^0 is larger and the barrier is smaller. So the ET is fast and at the same time the fluorescence is blue-shifted. In Figure 12c the configuration corresponds to a lower E_{0-0} and vibronic states are excited. The ET from the vibrationally excited states could be similar to that in Figure 12b. As the vibrational relaxation and redistribution in the excited state is rather fast (around 100−500 fs[43−46]) some of the configurations will relax to the bottom of the excited potential surface. For the relaxed configurations the barrier for ET is larger. So in the relaxed configurations ET is slow and at the same time the fluorescence is red-shifted. At the longest wavelength of observation (at 986 and 940 nm in DMA and 927 nm in AN) a small rise of the fluorescence signal is observed near the time zero (Figure 6). This could be attributed to relaxation processes such as vibrational relaxation, reactant motion, or solvation.

Finally we wish to mention the difference in solvation dynamics observed by dynamic Stokes shift and the configuration-dependent reaction currently observed in this study. In the solvation process the excitation energy is stabilized due to orientational motion of the solvent molecules, and the fluorescence spectrum shifts to the red.[31−33] Accordingly, the fluorescence decay at the blue edge of the fluorescence spectrum is accompanied with the rise at the red part of the spectrum. If the lifetime of the excited state is shortened by extra relaxation processes like ET, then it is not easy to separate these two processes. If solvation is slower than ET, then no large wavelength dependence should be observed due to solvation. If solvation is faster or comparable with ET rate then some wavelength dependence should be observed due only to solvation and a rising part should be clearly observed. In the present case, however, we do not observe any fluorescence rise except for a tiny contribution at the most red wavelength. Because of the properties of the ground and excited states of OX1 due to a small Stokes shift (4.1), we expect a small solvation effect. This is supported by the very small solvation effect seen in the inert solvent ClNP (Figure 8).

The most interesting point of the present system is that the anilines are not only a solvent but also a reactant, and competition between solvation and reaction could take place at very early stage of dynamics. Even though there is no large solvation effect, there should be a large dependence of the ET rate from mutual orientation and intermolecular distance for the reaction. The motions of the reactants change the barrier for the ET reaction through changes of reorganization energy and E_{0-0}. This motion is schematically shown in Figure 12a by arrows. If the ET rate is slower than this motion, then different configurations will be efficiently mixed by the motion and a smaller wavelength dependence will be expected. That is why the wavelength dependence in AN is smaller than in DMA. Thus, the observed wavelength dependence is assigned to fluorescence from different configurations of reactants highlighted by ultrafast ET reactions.

Acknowledgment. The authors are thankful to Dr. E. Slobodchikov for helping with the Cr:F laser and Mr. Grigorii Rubtsov for writing a program for data acquisition. The authors also thank Prof. K. Tominaga, Dr. S. Kumazaki, and Dr. K. Ohta for support of the work. We thank Prof. K. Ando (Tsukuba University) for fruitful discussions.

References and Notes

(1) Kosower, E. M.; Huppert, D. *Annu. Rev. Phys. Chem.* **1986**, *37*, 127.

(2) Barbara, P.; Jarzeba, W. *Adv. Photochem.* **1990**, *15*, 1.

(3) Wiederrecht, G. P.; Watanabe, S.; Wasielewski, M. R. *Chem. Phys.* **1993**, *176*, 601.

(4) Simon, J. D.; Doolen, R. *J. Am. Chem. Soc.* **1992**, *114*, 4861.
(5) Kobayashi, T.; Takagi, Y.; Kandori, H.; Kemnitz, K.; Yoshihara, K. *Chem. Phys. Lett.* **1991**, *180*, 416.
(6) Tominaga, K.; Kliner, D. A. V.; Johnson, A. E.; Levinger, N. E.; Barbara, P. F. *J. Chem. Phys.* **1993**, *98*, 1228.
(7) Mataga, N.; Asahi, T.; Kanda, Y.; Okada, T.; Kakitani, T. *Chem. Phys. Lett.* **1988**, *127*, 249.
(8) Tominaga, K.; Walker, G. C.; Jarzeba, W.; Barbara, P. F. *J. Phys. Chem.* **1991**, *95*, 10475.
(9) Kang, T. J.; Jarzeba, W.; Barbara, P. F.; Fonseca, T. *Chem. Phys.* **1990**, *149*, 81.
(10) Wang, C,; Akhremitchev, B.; Walker, G. C. *J. Phys. Chem. A.* **1997**, *101*, 2735.
(11) Wynne, K.; Galli, C.; Hochstrasser, R. M. *J. Chem. Phys.* **1994**, *100*, 4797.
(12) Jimenez, R.; Dikshit, S. N.; Bradforth, S. E.; Fleming, G. R. *J. Phys. Chem.* **1996**, *100*, 6825.
(13) Marcus, R. A. *J. Chem. Phys.* **1956**, *24*, 979; Marcus, R. A. *J. Chem. Phys.* **1963**, *38*, 1858; Marcus, R. A. *J. Chem. Phys.* **1965**, *43*, 679.
(14) Levich, V. G.; Dogonadze, R. R. *Dokl. Acad. Nauk SSSR* **1959**, *124*, 123, (*Proc. Acad. Sci. Phys. Chem. Sect.* **1959**, *124*, 9).
(15) Jortner, J. *J. Chem. Phys.* **1976**, *64*, 4860.
(16) Jortner, J.; Bixon, M. *J. Chem. Phys.* **1988**, *88*, 167.
(17) Zusman, L. D. *Chem. Phys.* **1983**, *80*, 29.
(18) Sumi, H.; Marcus, R. A. *J. Chem. Phys.* **1986**, *84*, 4894.
(19) Rips, I.; Jortner, J. *J. Chem. Phys.* **1987**, *87*, 2090.
(20) Calef, D. F.; Wolynes, P. G. *J. Phys. Chem.* **1983**, *87*, 3387.
(21) Tominaga, K.; Walker, G. C.; Kang, T. J.; Barbara P. F.; Fonseca, T. *J. Phys. Chem.* **1991**, *95*, 10485.
(22) Walker, G. C.; Akesson, E.; Johnson, A. E.; Levinger, N. E.; Barbara, P. F. *J. Phys. Chem.* **1992**, *96*, 3728.
(23) Yoshihara, K. In *Ultrafast processes in chemistry and photobiology*; El-Saed, M. A., Tanaka, I., Molin, Y., Eds.; Blackwell Science: Oxford, 1995.
(24) Yartsev, A.; Nagasawa, Y.; Douhal, A.; Yoshihara, K. *Chem. Phys. Lett.* **1993**, *207*, 546.
(25) Kandori, H.; Kemnitz, K.; Yoshihara, K. *J. Phys. Chem.* **1992**, *96*, 8042.
(26) Yoshihara, K.; Nagasawa, Y.; Yartsev, A.; Kumazaki, S.; Kandori, H.; Johnson, A. E.; Tominaga, K. *J. Photochem. Photobiol. A: Chem.* **1994**, *80*, 169.
(27) Slobodchikov, E.; Ma, J.; Kamalov, V.; Tominaga, K.; Yoshihara, K. *Opt. Lett.* **1996**, *21*, 354.
(28) Dewar, M. J. S.; Zoebisch, E. G.; Healy, E. F.; Stewart, J. J. P. *J. Am. Chem. Soc.* **1985**, *107*, 3902.
(29) Seel, M.; Enleitner, S.; Zinth, W. *Chem. Phys. Lett.* **1997**, *275*, 363.
(30) Renn, A.; Bucher, S. E.; Meixner, A. J.; Meister E. C.; Wild, U. P. *J. Lumin.* **1988**, *39*, 181.
(31) Maroncelli, M.; Fleming, G. R. *J. Chem. Phys.* **1988**, *89*, 5044.
(32) Carter, E. A.; Hynes J. T. *J. Chem. Phys.* **1991**, *94*, 5961.
(33) Fonseca, T.; Ladanyi, B. M. *J. Phys. Chem.* **1991**, *95*, 2116.
(34) Horng, M. L.; Gardecki, J. A.; Papazyan, A.; Maroncelli, M. *J. Phys. Chem.* **1995**, *99*, 17311.
(35) Rosenthal, S. L.; Xie, X.; Du, M.; Fleming, G. R. *J. Chem. Phys.* **1991**, *95*, 4715.
(36) Smith, N. A.; Lin, S.; Meech, S. R.; Shirota, H.; Yoshihara, K. *J. Phys. Chem. A* **1997**, *101*, 9578.
(37) Smith, N. A.; Meech, S. R.; Rubtsov, I. V.; Yoshihara, K. *Chem. Phys. Lett.*, in press.
(38) Pal, H.; Nagasawa, Y.; Tominaga, K.; Kumazaki, S.; Yoshihara, K. *J. Chem. Phys.* **1995**, *102*, 7758.
(39) Eads, D. D.; Dismer, B. G.; Fleming, G. R. *J. Chem. Phys.* **1990**, *92*, 1136.
(40) Shirota, H.; Pal, H.; Tominaga, K.; Yoshihara, K. *J. Phys. Chem. A* **1998**, *102*, 3089.
(41) Winkler, J. R.; Gray, H. B. *Chem. Rev.* **1992**, *92*, 369.
(42) Marcus, R. A.; Sutin, N. *Biochim. Biophys. Acta* **1985**, *811*, 265.
(43) Fragnito, H. L.; Bigot, J.-Y.; Becker, P. C.; Shank, C. V. *Chem. Phys. Lett.* **1989**, *160*, 101.
(44) Mokhtari, A.; Chebira, A.; Chesnoy, J. *J. Opt. Soc. Am.* **1990**, *7*, 1551.
(45) Laermer, F.; Elsaesser, T.; Kaiser, W. *Chem. Phys. Lett.* **1989**, *156*, 381.
(46) Elsaesser, T.; Kaiser, W. *Annu. Rev. Phys. Chem.* **1991**, *42*, 83.